Singlet Fission

International Edition: DOI: 10.1002/anie.201601421
German Edition: DOI: 10.1002/ange.201601421

High-Yield Excited Triplet States in Pentacene Self-Assembled Monolayers on Gold Nanoparticles through Singlet Exciton Fission

Daiki Kato, Hayato Sakai, Nikolai V. Tkachenko, and Taku Hasobe**

Abstract: *One of the major drawbacks of organic-dye-modified self-assembled monolayers on metal nanoparticles when employed for efficient use of light energy is the fact that singlet excited states on dye molecules can be easily deactivated by means of energy transfer to the metal surface. In this study, a series of 6,13-bis(triisopropylsilylethynyl)pentacene–alkanethiolate monolayer protected gold nanoparticles with different particle sizes and alkane chain lengths were successfully synthesized and were employed for the efficient generation of excited triplet states of the pentacene derivatives by singlet fission. Time-resolved transient absorption measurements revealed the formation of excited triplet states in high yield (172 ± 26 %) by suppressing energy transfer to the gold surface.*

The construction of organic–inorganic hybrid materials is of great interest for both fundamental and applied research.[1] A major research topic is light energy conversion through photoinduced processes, such as electron and energy transfer.[1a,2] Therefore, two- and three-dimensional self-assembled monolayers (SAMs) of organic dyes on metal surfaces and nanoparticles are highly promising as photofunctional nanomaterials.[3] However, a major problem for organic-dye-modified SAMs on metal surfaces is the significant deactivation pathway of the dye-molecule excited states caused by fast dipole–surface energy transfer (or electron transfer).[1b,4] In these cases, more than 90 % of fluorescence (FL) is quenched and the formation of excited triplet states is negligible. Therefore, the formation of long-lived excited triplet states on metal surfaces in high yield is favorable for various applications using photoinduced processes.

The generation of efficient singlet fission (SF) on gold nanoparticles (GNP) is a promising method to overcome the above-mentioned problem. We can describe SF as a spin-allowed process in which one singlet exciton splits into two triplet excitons.[5] This peculiar photophysical process is mainly detected in crystalline and aggregate states of organic molecules,[6] although studies have recently reported the occurrence of SF in covalently linked molecular dyads[7] and in liquid-phase solution processes.[8] Efficient SF requires that the energy of the lowest-lying singlet excited state $E(S_1)$ is larger than, or close to, the energy of two triplet excited states $2E(T_1)$ (that is, $E(S_1) \geq 2E(T_1)$). Among polyacenes, pentacenes meet the above requirement and have large coupling energies as compared to the other acene derivatives, such as tetracene and hexacene.[6d,9] Recent results also suggest significant interplay between the excited singlet state (S_1) and correlated triplet states (^{1}(TT)) through the intermediate charge-transfer (CT) state in acene derivatives.[5b,10] According to recent results,[6c,d,7b] ultrafast SF (about 10^{13}–10^{11} s^{-1}) occurs in dimers and crystals of pentacenes. Consequently, closely packed TP-modified SAMs (TP = 6,13-bis(triisopropylsilylethynyl)pentacene) are expected to form long-lived triplet states in high yield through ultrafast SF processes.

In this Communication, we report the first synthesis and investigation of the photophysical properties of TP–alkanethiolate monolayer-protected gold nanoparticles (TP-C*n*-*X*-MPCs). As shown in Figure 1, a series of TP-C*n*-*X*-MPCs with two different particle sizes (where *X* indicates small (*S*) and large (*L*) sizes, respectively) and two different chain lengths

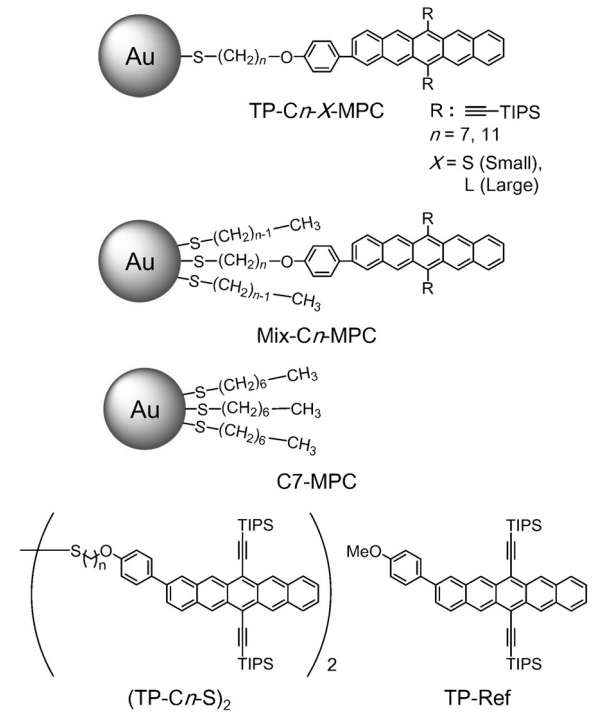

Figure 1. The chemical structures of TP-C*n*-*X*-MPC (*X* = *S* (small), *L* (large)), Mix-C*n*-MPC, C*n*-MPC, (TP-C*n*-S)$_2$, and TP-Ref used in this study.

[*] D. Kato, Dr. H. Sakai, Prof. T. Hasobe
Department of Chemistry
Faculty of Science and Technology, Keio University
Yokohama, Kanagawa 223-8522 (Japan)
E-mail: hasobe@chem.keio.ac.jp
Prof. N. V. Tkachenko
Department of Chemistry and Bioengineering
Tampere University of Technology
P.O. Box 541, 33101 Tampere (Finland)
E-mail: nikolai.tkachenko@tut.fi

Supporting information for this article can be found under: http://dx.doi.org/10.1002/anie.201601421.

($n = 7$, 11) were synthesized. Moreover, we also observed efficient SF, which is the first time that this has been detected on metal nanoparticles. By changing these structural parameters, we successfully controlled the rate constants and quantum yields of SF by suppressing the fast energy transfer to GNP.

The chemical structures of TP disulfides (TP-C*n*-S)$_2$, TP-C*n*-*X*-MPCs, and TP-Ref (the reference monomer) are shown in Figure 1. The TP-C*n*-*S*-MPC was synthesized following a reported method.[11] The synthesis of mixed TP/alkanethiolate MPCs (denoted Mix-C*n*-MPC; molecular ratio of TP:alkanethiol on the GNP = 1:2; see Table S3 in the Supporting Information), and pristine alkanethiolate MPC (C7-MPC) were performed using the same procedures. The synthetic procedures and characterization data are shown in the experimental section and Figures S1–S17 in the Supporting Information.

The TEM images and size distributions of TP-C11-*X*-MPC are shown in Figure 2 (see Figures S18–S21 for data for TP-C7-*X*-MPC and the reference systems). The mean diameters (R_{CORE}) of TP-C11-*S*-MPC and TP-C11-*L*-MPC are

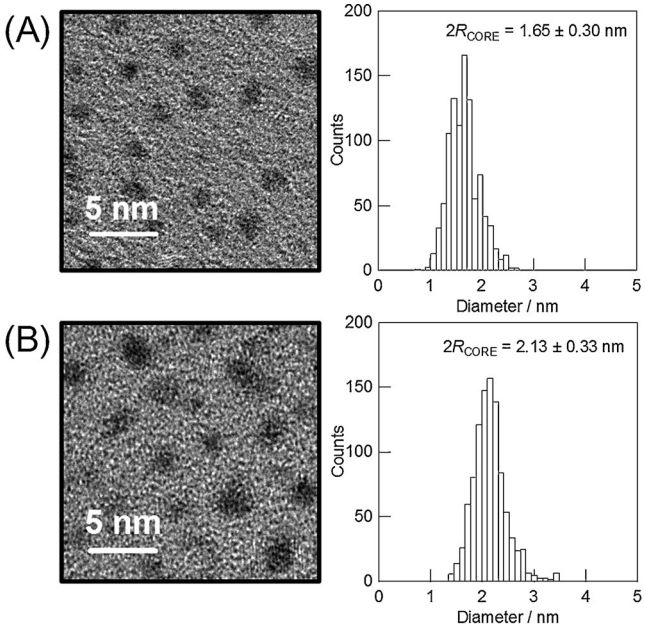

Figure 2. TEM images (left) and size distributions (right) of A) TP-C11-*S*-MPC and B) TP-C11-*L*-MPC.

1.65 ± 0.30 nm and 2.13 ± 0.33 nm, respectively. These values are very similar to those of the TP-C7-*X*-MPC systems (Tables S1, S2). The reported "spherical model" by Murray et al.[12] predicted that the core of TP-C11-*S*-MPC and TP-C11-*L*-MPC contains 158 and 338 Au atoms, respectively. Moreover, based on the elemental analysis results (Table S1), there are 51 (TP-C11-*S*-MPC) and 75 (TP-C11-*L*-MPC) TP molecules on one GNP (see Table S2 for the similar results obtained for TP-C7-*X*-MPC). In addition, the coverage ratios of TP units (γ) to surface Au atoms in TP-C11-*S*-MPC and TP-C11-*L*-MPC are 63% and 51%, respectively (for the reference materials TP-C7-*S*-MPC $\gamma = 68\%$, TP-C7-*L*-MPC $\gamma = 55\%$). The γ values of Mix-C7-MPC and Mix-C11-MPC are 17% and 26%, respectively (Table S3).

Steady-state absorption and FL spectra of TP-C*n*-*X*-MPCs and TP-Ref were measured in toluene (Figure 3; Figures S22–S25). In the absorption spectra (Figure 3A), the spectral profile of TP-C11-*S*-MPC (solid line) corresponds well to that of TP-Ref (dashed line). The slight increased absorption of the baseline is due to the absorption of GNP

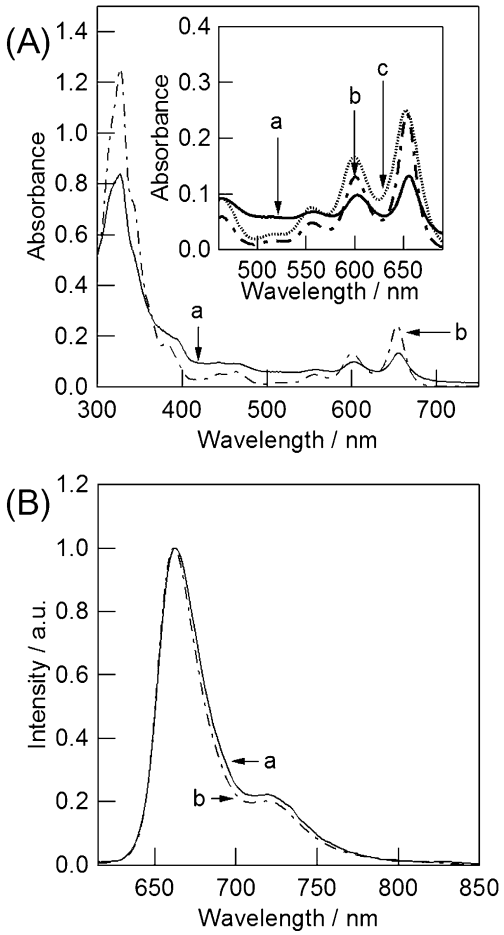

Figure 3. A) Absorption spectra of a) TP-C11-*S*-MPC (about 0.5 mg mL^{-1}; solid line) and b) TP-Ref (10 μM; dashed line), as well as the c) excitation spectrum of TP-C11-*S*-MPC (dotted line) in toluene (monitored at $\lambda_{em} = 722$ nm). B) Fluorescence spectra of a) TP-C11-*S*-MPC (solid line) and b) TP-Ref (dashed line) in toluene ($\lambda_{ex} = 600$ nm).

including surface plasmon resonance (SPR) effects.[13] The relative ratio of the absorption of TP units to GNP decreased with increasing GNP sizes because of the decreased γ values (see above; Figure S22). Alternatively, this effect may be due to the increased absorption coefficient of the larger sized GNP, in accordance with previous theoretical and experimental results.[14]

The FL of TP-C11-*S*-MPC was strongly quenched relative to TP-Ref because of SF (see below). To compare the emission spectral profiles, the FL spectra of TP-C11-*S*-MPC (solid line) and TP-Ref (dashed line) were normalized in Figure 3B. The FL excitation spectrum was also recorded

(Figure 3A, dotted line) in order to carefully check the FL species of TP-C11-*S*-MPC. The excitation spectrum is clearly coincident with the corresponding absorption spectrum (Figure 3A, solid line), which indicates that the emission arises from the excited singlet states of TP units only. The FL spectral trends of other systems were also similar to the above results (Figures S24, S25).

Time-resolved transient absorption spectra of TP-C*n*-*X*-MPCs in toluene were measured by femtosecond (fs) laser flash photolysis to examine the ultrafast photodynamics. The measurements of transient spectra were performed using a 600 or 653 nm fs laser pulse (full width at half maximum, fwhm = 100 fs), which was used to excited the TP units. The excitation density was decreased to the level at which excitation of more than two TP molecules attached to one GNP can be neglected (see the captions of Figures S26 and S27). Figures 4A, B show the transient spectra of TP-C11-*S*-MPC. After laser pulse excitation, the triplet–triplet (T–T) absorption band for the TP units at about $\lambda = 520$ nm develops, whereas the singlet–singlet (S–S) absorption band at about $\lambda = 630$ nm decays. The T–T absorption band of the TP units was separately assigned by using the energy transfer from anthracene to TP-Ref (Figure S28). The S–S absorption spectrum of TP is shown in Figure S29.

Figure 4C shows the time profiles at $\lambda = 513$ and 628 nm for TP-C11-*S*-MPC. The results for TP-C*n*-*X*-MPC are shown in Figures S26–S34. The gradual rise at $\lambda = 513$ nm is attributable to the formation of excited triplet states by means of SF, whereas the contrasting decay at 628 nm is mainly due to deactivation of the excited singlet states of the TP units. The T–T absorption was also detected in TP-C11-*L*-MPC (Figure S30). These trends were quite similar for TP-C7-*X*-MPC systems. Therefore, a closer distance between the nearest two TP units on GNP (that is, small particle systems) is favorable for efficient SF to occur. In addition, no S–S annihilation occurred at the higher excitation energy (Figure S26,S27).

Figure 4D also shows the decay component spectra of TP-C11-*S*-MPC obtained by global fitting of the transient absorption data to a four-exponential model.[15] The decay component spectra of TP-C*n*-*X*-MPC are shown in Figure S33. A model with four exponents was needed to obtain reasonable sigma values and consistent fits at all wavelengths, and resulted in two pairs of decay component spectra indicating the formation of a transient band at $\lambda = 520$ nm (1.7 ps and 21 ps) and a subsequent decay (590 ps and 13 ns). It should be noted that the longest delay time of the instrument is 6 ns, and thus a 13 ns lifetime is longer than can be determined using this method (see the section on nanosecond flash photolysis).

Two of the fast components (1.7 ps and 21 ps) have negative bands at around $\lambda = 513$ nm, indicating the formation of the transient absorption band at this wavelength. Despite the major similarities of the 1.7 ps and 21 ps component spectra, the spectra have very different effects on transient absorption dynamics in the $\lambda = 540$–600 nm range and can be clearly separated. However, the latter component is due to the formation of an intermediate state with a distinct absorption band at $\lambda = 513$ nm, which is a characteristic feature of the triplet state. At least two explanations can be offered for this "biphasic" triplet state. First, it has been reported that SF is mediated by a CT state in a pentacene dimer which results in biexponential formation of the triplet-state absorption band.[7a] Second, TP-C*n*-*X*-MPCs are essentially heterogeneous systems and different TP aggregates can be formed spontaneously, which may lead to a difference in SF time constants in particular and different excitation relaxation dynamics in general. Additionally, some contribution from the plasmon relaxation dynamics on GNPs on the component spectra cannot be excluded (Figure S34).[16]

To verify the pump–probe results and component assignment, the FL decays were measured using the fs up-conversion technique (Figure S35). Similar biexponential FL decays were detected with

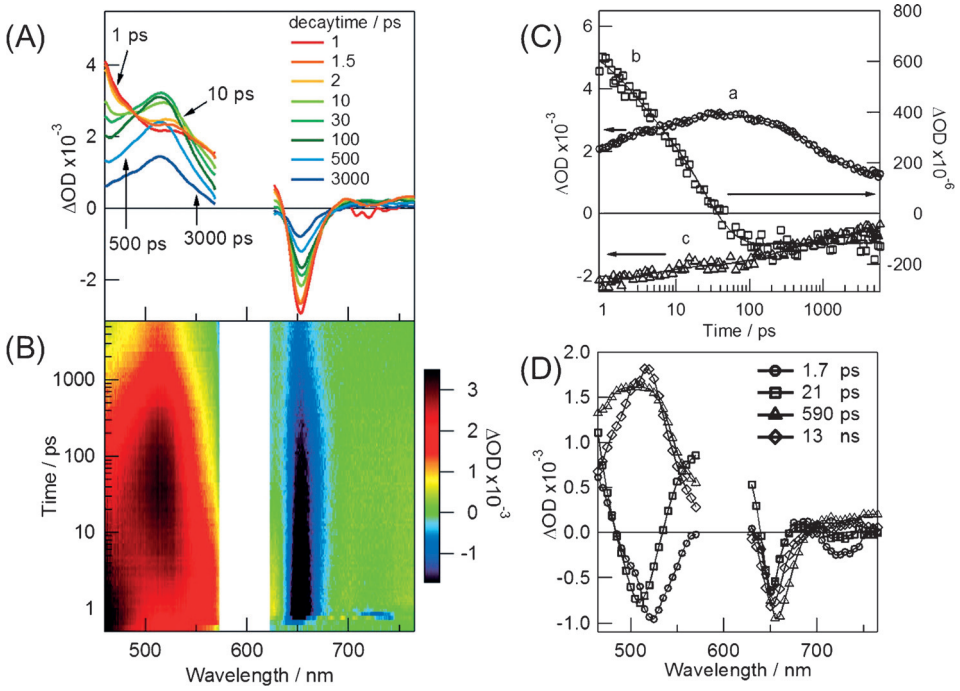

Figure 4. A) Femtosecond transient absorption spectra and B) differential absorption spectral changes of TP-C11-*S*-MPC in toluene at room temperature. C) Time profiles of TP-C11-*S*-MPC at $\lambda = 513$ nm (a; ○), 628 nm (b; □) and 660 nm (c; △). In (C), plots (a) and (c) relate to the left-hand vertical axis, whereas plot (b) should be interpreted using the right-hand vertical axis. D) Decay component spectra of TP-C11-*S*-MPC obtained by a global four-exponential fit of the transient absorption data presented in (B). $\lambda_{ex} = 600$ nm, low laser intensity ($< 30\ \mu J\ cm^{-2}$).

time constants close to those obtained from fs transient analysis. This can be interpreted in favor of the second hypothesis, heterogeneity of aggregates, since an intermediate CT state is expected to have no or much weaker emission, and in an ideal case should lead to monoexponential FL decay. Similar behavior was detected in TP-C7-*S*-MPC.

The triplet quantum yields (Φ_T) were evaluated using previously reported methods[7b,8] and are summarized in Table 1. Details of the calculation processes are shown in the Supporting Information (see Tables S4,S5). The maximum Φ_T values obtained were $172 \pm 26\,\%$ and $157 \pm 17\,\%$ in TP-C11-*S*-MPC and TP-C7-*S*-MPC, respectively. The Φ_T values decrease with increasing GNP sizes, probably because of the smaller γ value of TP units on smaller GNPs. In contrast, the Φ_T value of TP-C7-*S*-MPC ($157 \pm 17\,\%$) is slightly smaller than that of TP-C11-*S*-MPC. To further examine the alkyl chain length effects on the rate constants of direct energy transfer to GNP without SF, we measured the singlet lifetimes of Mix-C7-MPC and Mix-C11-MPC by fs transient absorption and FL lifetime measurement. It should be emphasized that no SF was detected in either Mix-C7-MPC or Mix-C11-MPC because of the low surface coverages, indicating that the Au atom does not contribute to the singlet–triplet conversion (Figures S36, S37). The lifetimes of Mix-C7-MPC and Mix-C11-MPC were determined to be 71 ps and 150 ps, respectively (Figures S36, S38), indicating that the energy-transfer process is dependent on the alkyl chain lengths, which agrees with the previously reported trend.[13]

Table 1: Lifetimes of excited singlet states (τ_S), rate constants of singlet fission (k_{SF}), and quantum yields of excited triplet states (Φ_T).

Compound	τ_S [ps] (k_{S1} [s^{-1}])	k_{SF} [s^{-1}][c]	Φ_T [%][d]
TP-Ref	1.5×10^{4}[a] (6.7×10^{7})	–	1.5[e]
TP-C7-*S*-MPC	24[b] (4.1×10^{10})	2.7×10^{10}	157 ± 17[f]
TP-C7-*L*-MPC	54[b] (1.9×10^{10})	5.0×10^{9}	77 ± 15[f]
TP-C11-*S*-MPC	21[b] (4.8×10^{10})	4.1×10^{10}	172 ± 26[f]
TP-C11-*L*-MPC	110[b] (9.1×10^{9})	2.4×10^{9}	34 ± 4[f]
Mix-C7-MPC	71[a] (1.4×10^{10})	–	–
Mix-C11-MPC	150[b] (6.7×10^{9})	–	–

[a] Estimated by picosecond FL lifetime measurements (see Figures S38, S39). [b] Estimated by decay component lifetimes (fs laser flash photolysis). [c] $k_{SF} = 1/\tau$(TP-C*n*-*X*-MPC) $- 1/\tau$(Mix-C*n*-MPC). [d] Details of the calculation processes are shown in the Supporting Information. [e] Estimated by nanosecond laser flash photolysis. [f] Estimated by fs laser flash photolysis.

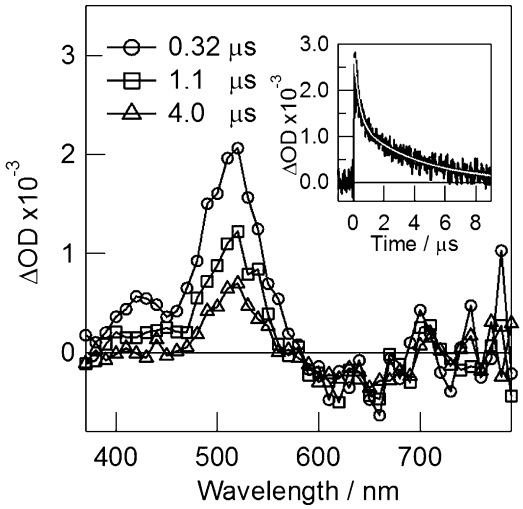

Figure 5. Nanosecond transient absorption spectra of TP-C11-*S*-MPC in toluene at room temperature ($\lambda_{ex} = 532$ nm). Inset: the decay profile of TP-C11-*S*-MPC monitoring at $\lambda = 510$ nm (black line) and the fitted curve (white line).

Finally, nanosecond transient absorption spectra of TP-C*n*-*X*-MPCs systems were measured to investigate the excited triplet states over a longer time range. Figure 5 shows the transient absorption spectra and decay profile of TP-C11-*S*-MPC. The spectra of the other systems are shown in Figures S40–S43. We can clearly observe T–T absorption of the TP units at about $\lambda = 510$ nm and that the triplet species has not fully decayed up to the microsecond timescale.

In conclusion, we present the first synthesis of a series of TIPS-pentacene–alkanethiolate monolayer protected gold nanoparticles with different particle sizes and alkyl chain lengths. High triplet quantum yields (for TP-C11-*S*-MPC, $\Phi_T = 172 \pm 26\,\%$) were measured. This study is the first observation of SF on metal nanoparticles and provides a novel approach for the control of excited-state dynamics on monolayer protected gold nanoparticles. This strategy may provide potential for the development of future applications, such as light energy conversion.

Acknowledgements

This work was partially supported by Grants-in-Aid for Scientific Research (Nos. 26286017, 26620159, 15H01003 "π-System Figuration", and 15H01094 "Photosynergetics" to T.H.).

Keywords: gold · nanoparticles · pentacene · self-assembled monolayers · singlet fission

How to cite: *Angew. Chem. Int. Ed.* **2016**, *55*, 5230–5234
Angew. Chem. **2016**, *128*, 5316–5320

[1] a) E. W. McFarland, J. Tang, *Nature* **2003**, *421*, 616–618; b) T. L. Jennings, M. P. Singh, G. F. Strouse, *J. Am. Chem. Soc.* **2006**, *128*, 5462–5467; c) H. I. Park, S. Lee, J. M. Lee, S. A. Nam, T. Jeon, S. W. Han, S. O. Kim, *ACS Nano* **2014**, *8*, 10305–10312.

[2] a) H. Choi, Y.-S. Chen, K. G. Stamplecoskie, P. V. Kamat, *J. Phys. Chem. Lett.* **2015**, *6*, 217–223; b) T. Hasobe, H. Imahori, P. V. Kamat, T. K. Ahn, S. K. Kim, D. Kim, A. Fujimoto, T.

Hirakawa, S. Fukuzumi, *J. Am. Chem. Soc.* **2005**, *127*, 1216 – 1228; c) S. Fukuzumi, Y. Yamada, T. Suenobu, K. Ohkubo, H. Kotani, *Energy Environ. Sci.* **2011**, *4*, 2754 – 2766.

[3] a) M.-C. Daniel, D. Astruc, *Chem. Rev.* **2004**, *104*, 293 – 346; b) D. A. Hines, P. V. Kamat, *ACS Appl. Mater. Interfaces* **2014**, *6*, 3041 – 3057; c) M. Tabachnyk, B. Ehrler, S. Gélinas, M. L. Böhm, B. J. Walker, K. P. Musselman, N. C. Greenham, R. H. Friend, A. Rao, *Nat. Mater.* **2014**, *13*, 1033 – 1038.

[4] a) A. Kotiaho, R. Lahtinen, A. Efimov, H.-K. Metsberg, E. Sariola, H. Lehtivuori, N. V. Tkachenko, H. Lemmetyinen, *J. Phys. Chem. C* **2010**, *114*, 162 – 168; b) G. Santosh, E. Shirman, H. Weissman, E. Shimoni, I. Pinkas, Y. Rudich, B. Rybtchinski, *J. Phys. Chem. B* **2010**, *114*, 14389 – 14396; c) B. I. Ipe, K. G. Thomas, S. Barazzouk, S. Hotchandani, P. V. Kamat, *J. Phys. Chem. B* **2002**, *106*, 18 – 21; d) F. Cannone, G. Chirico, A. R. Bizzarri, S. Cannistraro, *J. Phys. Chem. B* **2006**, *110*, 16491 – 16498; e) H. Imahori, M. Arimura, T. Hanada, Y. Nishimura, I. Yamazaki, Y. Sakata, S. Fukuzumi, *J. Am. Chem. Soc.* **2001**, *123*, 335 – 336.

[5] a) M. B. Smith, J. Michl, *Chem. Rev.* **2010**, *110*, 6891 – 6936; b) M. B. Smith, J. Michl, *Annu. Rev. Phys. Chem.* **2013**, *64*, 361 – 386; c) J. Lee, P. Jadhav, P. D. Reusswig, S. R. Yost, N. J. Thompson, D. N. Congreve, E. Hontz, T. Van Voorhis, M. A. Baldo, *Acc. Chem. Res.* **2013**, *46*, 1300 – 1311; d) M. C. Hanna, A. J. Nozik, *J. Appl. Phys.* **2006**, *100*, 074510.

[6] a) E. A. Margulies, Y.-L. Wu, P. Gawel, S. A. Miller, L. E. Shoer, R. D. Schaller, F. Diederich, M. R. Wasielewski, *Angew. Chem. Int. Ed.* **2015**, *54*, 8679 – 8683; *Angew. Chem.* **2015**, *127*, 8803 – 8807; b) A. J. Musser, M. Maiuri, D. Brida, G. Cerullo, R. H. Friend, J. Clark, *J. Am. Chem. Soc.* **2015**, *137*, 5130 – 5139; c) M. W. B. Wilson, A. Rao, B. Ehrler, R. H. Friend, *Acc. Chem. Res.* **2013**, *46*, 1330 – 1338; d) S. R. Yost, J. Lee, M. W. B. Wilson, T. Wu, D. P. McMahon, R. R. Parkhurst, N. J. Thompson, D. N. Congreve, A. Rao, K. Johnson, M. Y. Sfeir, M. G. Bawendi, T. M. Swager, R. H. Friend, M. A. Baldo, T. Van Voorhis, *Nat. Chem.* **2014**, *6*, 492 – 497; e) J. N. Schrauben, Y. Zhao, C. Mercado, P. I. Dron, J. L. Ryerson, J. Michl, K. Zhu, J. C. Johnson, *ACS Appl. Mater. Interfaces* **2015**, *7*, 2286 – 2293.

[7] a) J. Zirzlmeier, D. Lehnherr, P. B. Coto, E. T. Chernick, R. Casillas, B. S. Basel, M. Thoss, R. R. Tykwinski, D. M. Guldi, *Proc. Natl. Acad. Sci. USA* **2015**, *112*, 5325 – 5330; b) S. N. Sanders, E. Kumarasamy, A. B. Pun, M. T. Trinh, B. Choi, J. Xia, E. J. Taffet, J. Z. Low, J. R. Miller, X. Roy, X. Y. Zhu, M. L. Steigerwald, M. Y. Sfeir, L. M. Campos, *J. Am. Chem. Soc.* **2015**, *137*, 8965 – 8972; c) J. C. Johnson, A. J. Nozik, J. Michl, *Acc. Chem. Res.* **2013**, *46*, 1290 – 1299; d) S. Lukman, A. J. Musser, K. Chen, S. Athanasopoulos, C. K. Yong, Z. Zeng, Q. Ye, C. Chi, J. M. Hodgkiss, J. Wu, R. H. Friend, N. C. Greenham, *Adv. Funct. Mater.* **2015**, *25*, 5452 – 5461.

[8] B. J. Walker, A. J. Musser, D. Beljonne, R. H. Friend, *Nat. Chem.* **2013**, *5*, 1019 – 1024.

[9] a) E. Busby, T. C. Berkelbach, B. Kumar, A. Chernikov, Y. Zhong, H. Hlaing, X. Y. Zhu, T. F. Heinz, M. S. Hybertsen, M. Y. Sfeir, D. R. Reichman, C. Nuckolls, O. Yaffe, *J. Am. Chem. Soc.* **2014**, *136*, 10654 – 10660; b) T. Minami, M. Nakano, *J. Phys. Chem. Lett.* **2012**, *3*, 145 – 150.

[10] a) D. Beljonne, H. Yamagata, J. L. Bredas, F. C. Spano, Y. Olivier, *Phys. Rev. Lett.* **2013**, *110*, 226402; b) N. Monahan, X. Y. Zhu, *Annu. Rev. Phys. Chem.* **2015**, *66*, 601 – 618.

[11] M. Brust, M. Walker, D. Bethell, D. J. Schiffrin, R. Whyman, *J. Chem. Soc. Chem. Commun.* **1994**, 801 – 802.

[12] R. H. Terrill, T. A. Postlethwaite, C.-h. Chen, C.-D. Poon, A. Terzis, A. Chen, J. E. Hutchison, M. R. Clark, G. Wignall, J. D. Londono, R. Superfine, M. Falvo, C. S. Johnson, Jr., E. T. Samulski, R. W. Murray, *J. Am. Chem. Soc.* **1995**, *117*, 12537 – 12548.

[13] H. Imahori, Y. Kashiwagi, Y. Endo, T. Hanada, Y. Nishimura, I. Yamazaki, Y. Araki, O. Ito, S. Fukuzumi, *Langmuir* **2004**, *20*, 73 – 81.

[14] J. Yguerabide, E. E. Yguerabide, *Anal. Biochem.* **1998**, *262*, 137 – 156.

[15] B. Pelado, F. Abou-Chahine, J. Calbo, R. Caballero, P. de la Cruz, J. M. Junquera-Hernández, E. Ortí, N. V. Tkachenko, F. Langa, *Chem. Eur. J.* **2015**, *21*, 5814 – 5825.

[16] T. S. Ahmadi, S. L. Logunov, M. A. El-Sayed, *J. Phys. Chem.* **1996**, *100*, 8053 – 8056.

Received: February 9, 2016
Published online: March 21, 2016

